0254-6124/2022/42(4)-0712-12 *Chin. J. Space Sci.* 空间科学学报

SHI Jiancheng, LÜ Daren, WANG Yu, DU Yan, PANG Yong, YANG Dongxu, WANG Xin, DONG Xiaolong, YANG Xiaofeng. Recent Progress of Earth Science Satellite Missions in China. *Chinese Journal of Space Science*, 2022, **42**(4): 712–723. DOI:10.11728/cjss2022.04.yg21

Recent Progress of Earth Science Satellite Missions in China

SHI Jiancheng[1] LÜ Daren[2] WANG Yu[3] DU Yan[4]
PANG Yong[5] YANG Dongxu[2] WANG Xin[2]
DONG Xiaolong[1] YANG Xiaofeng[3]

1(*National Space Science Center*, *Chinese Academy of Sciences*, *Beijing* 100190)

2(*Institute of Atmospheric Physics*, *Chinese Academy of Sciences*, *Beijing* 100029)

3(*Aerospace Information Research Institute*, *Chinese Academy of Sciences*, *Beijing* 100094)

4(*South China Sea Institute of Oceanology*, *Chinese Academy of Sciences*, *Guangzhou* 510301)

5(*Institute of Forest Resource Information Technique*, *Chinese Academy of Forestry*, *Beijing* 100091)

Abstract Earth Science from Space is an interdisciplinary discipline that studies the interactions, mechanisms, and evolution of the Earth system through space observation. In China, the national medium- to long-term civilian space infrastructure development plan and the space-science pilot project from the Chinese Academy of Sciences are two programs associated with advancing the Earth science from space. This paper reports recent scientific findings, developments and the status of the six missions. It is organized as the following sections: Introduction, two satellite missions that are already in orbit—the TanSat-1 for atmospheric CO_2 and the LuTan-1 for global surface deformation, a Terrestrial Ecosystem Carbon Inventory Satellite to be launched in 2022, and three missions that passed the Phase II study and planned for near future—the Ocean Surface Current multiscale Observation, the Terrestrial Water Resources Satellite. Climate and Atmospheric Components Exploring Satellites (CACES), followed by the conclusion.

Key words Earth science from space, Earth observation, Energy and water cycle, Carbon cycle, Human activities

Classified index V474.1

1 Introduction

Earth science is a fundamental discipline with strong practicality, and experiments and observations play an important role in promoting the development of the domain. For a long time, the observation of the Earth can only be limited to a few points or a small area, which has a substantial limitation for a comprehensive, comprehensive and overall study of the Earth. Small-scale conclusions usually cannot be mechanically extrapolated to large-scale. The development of satellite Earth observation technology has presented the Earth in a complete form to scientists and the public for the first time. China is one of the few nations that has been successful in developing a comprehensive Earth observation system. Since 2020, China has developed and launched several new satellites to support Earth science studies.

Received June 29, 2022
E-mail: shijiancheng@nssc.ac.cn

2 TanSat-1

Since CO_2 has been recognized as the most important anthropogenic greenhouse gas owing to its significant impact on global warming and climate change, there are a substantial number of studies that have focused on investigating the status of CO_2 in the atmosphere in the past and present, and how it will change in the future. In support of the upcoming global stocktake in 2023, we require a new method to verify how much human emissions impact the global carbon cycle and climate change.

The first Chinese carbon dioxide monitoring satellite mission, TanSat, which was supported by the Ministry of Science and Technology of China, the Chinese Academy of Sciences, and the China Meteorological Administration, was launched in December 2016 to monitor carbon dioxide (CO_2) concentrations in the atmosphere over the globe.

2.1 A New TanSat XCO_2 Data Product

The first TanSat global map of CO_2 dry-air mixing ratio (XCO_2) measurements over land was released as version 1 data product[1] with an accuracy of 2.11 ppmv (parts per million by volume)[2,3]. Unfortunately, it is not accurate enough to support estimation of anthropogenic CO_2 emissions in cities due to it has a 1–1.5 ppm gradient across the urban regions as has been shown from ground-based measurement in Paris. On TanSat 4th birthday coming this year, we introduce a new (version 2) TanSat global XCO_2 product that is approached by the Institute of Atmospheric Physics Carbon dioxide retrieval Algorithm for Satellite remote sensing (IAPCAS), and the European Space Agency (ESA) Climate Change Initiative plus (CCI^+) TanSat XCO_2 product by University of Leicester Full Physics (UoL-FP) retrieval algorithm[4]. The new TanSat XCO_2 data product is now retrieved by the Institute of Atmospheric Physics Carbon dioxide retrieval Algorithm for Satellite remote sensing (IAPCAS) using the O_2 A-band and CO_2 weak band together, after A new approach has been developed to improve the retrieval accuracy by optimizing the TanSat measured spectrum. The TanSat v2 XCO_2 data product can be obtained from the CASA TanSat data and science service*. The inter-comparison of TanSat XCO_2 retrieval between the two algorithms shows a good agreement for all TCCON overpass measurements with 34699 individual measurements. The dispersion between the two data products has a standard deviation of 1.28 ppmv, and there is a –0.35 ppmv overall bias between both, and this systematic error[5].

2.2 Global Carbon Flux Distribution Derived from TanSat-1

The new version of TanSat XCO_2 data has been applied to drive the TanSat's first estimates of the global distribution of carbon surface fluxes inferred from dry-air CO_2 column (XCO_2), by using an Ensemble Transform Kalman Filter (ETKF) data assimilation system coupled with the GEOS-Chem global chemistry transport model to optimally fit model simulations with the TanSat XCO_2 observations[6]. High posterior error reduction (30%–50%) compared with a priori fluxes indicates that assimilating satellite XCO_2 measurements provides highly effective constraints on global carbon flux estimation. The impacts of TanSat XCO_2 observations are also highlighted by significant spatiotemporal shifts in flux patterns over regions critical to the global carbon budget, such as tropical South America and China. An integrated global land carbon net flux of 6.71 ± 0.76 $GtC \cdot yr^{-1}$ over 12 months (May 2017 to April 2018) is estimated from the TanSat XCO_2 data, which is generally consistent with other inversions based on satellite data, such as the JAXA GOSAT and NASA OCO-2 XCO_2 retrievals. Further study attempts to estimate terrestrial Net Ecosystem Exchange (NEE) using TanSat XCO_2 retrievals based on the GEOS-Chem 4 D-Var data assimilation system and infer the global NEE from April 2017 to March 2018 using TanSat XCO_2 retrievals[7]. The estimates global NEE at –3.46 $PgC \cdot yr^{-1}$, evidently higher than the prior estimate and giving rise to an improved estimate of global atmospheric CO_2 growth rate.

2.3 SIFs Derived from TanSat-1

Solar-induced chlorophyll Fluorescence (SIF) is emitted during plant photosynthesis, and it is recognized as the ideal proxy for terrestrial Gross Primary Productivity (GPP) according to many laboratory and field experiments. In recent years, a large number of studies have shown that SIF can effectively improve the estimation of GPP and then promote the quantitive research of the global carbon sink. The first TanSat SIF map was ob-

*http://www.chinageoss.cn/tansat/index.html

tained by the SVD method[8]. A new TanSat SIF product is retrieved by a physical-based algorithm (IAPCAS/SIF), and this algorithm is based on the IAPCAS. The new TanSat SIF product is retrieved from two microwindows in the O_2 A-band, representing the SIF emission at 757 nm and 771 nm[9]. The new TanSat SIF data product can be obtained from the the Cooperation on the Analysis of carbon Satellites data (CASA) TanSat data and science service*. Comparing global distributions of SIF retrieved by IAPCAS/SIF from TanSat and OCO-2 shows the same spatial pattern for all seasons with gridded SIF difference less than 0.3 $W\cdot m^{-2}\cdot\mu m^{-1}\cdot sr^{-1}$[10]. The global distributions also agree well with the official OCO-2 SIF product with a difference less than 0.2 $W\cdot m^{-2}\cdot\mu m^{-1}\cdot sr^{-1}$. The retrieval uncertainty of seasonally gridded TanSat IAPCAS/SIF is less than 0.03 $W\cdot m^{-2}\cdot\mu m^{-1}\cdot sr^{-1}$ whereas the uncertainty of each sounding ranges from 0.1 to 0.6 $W\cdot m^{-2}\cdot\mu m^{-1}\cdot sr^{-1}$.

3 LuTan-1

LuTan-1 mission (referred as LT-1) is an innovative space borne Earth observation constellation. It contains two identical satellites that both carry an advanced full polarimetry L-band Synthetic Aperture Radar (SAR). The LT-1 A was successfully launched by the Long March-4 C carrier rocket on 26 January 2022, from the Jiuquan Satellite Launch Center (China). The LT-1 B was launched successfully on 27 February 2022. LT-1 is the first launched satellite mission in the "China National Civil Space Infrastructure Long-Term Development Plan (2015–2025)". The main tasks of LT-1 are global surface deformation measurement and Digital Elevation Model (DEM) acquisition. The data of LT-1 can also serve many industries such as land, earthquake, mapping, environment, disaster mitigation, forestry, *etc*.

The scientific objectives of LT-1 include global DEM acquirement, surface deformation measurement, biomass observation, and geological hazards monitoring and assessment. To meet the requirements of scientific objective, the satellite is designed to be in a sun-synchronous orbit with a high inclination of 97.8° at an altitude of around 607 km. The LT-1 A and LT-1 B satellites can work independently, and can also be used for dual-satellite collaborative imaging and Interferometric SAR (InSAR) applications. Each satellite equips an L-Band SAR as the main payload. It can provide an all-weather, day-and-night supply of images of the Earth's surface. The L-Band SAR operates in six imaging modes (Table 1) with different resolutions (down to 3 m) and coverages (up to 400 km). It provides the multi-polarization capability and very short revisit times. The revisit time of a single satellite of LT-1 is 8 days. The two-satellite constellation can offer a 4 days exact repeat cycle. Wide swath coverage and efficient revisit frequency will significantly facilitate the acquisition of time series images. In addition, the L-band has excellent coherence maintenance capability, which is of great significance for emergency management of disasters such as earthquakes and landslides.

The two satellites are expected to operate for 8 years in orbit. The duration of the mission is divided into two phases. In phase I, two satellites fly in a formation with a variable baseline, and the bistatic InSAR strip map mode is utilized to acquire the global digital elevation and terrain models with high accuracy and spatial resolution. In phase II, two satellites shall share the common reference orbit with a 180° orbital phasing difference. Land deformation with millimeter accuracy at a large scale can be measured using the differential InSAR technique. For high-precision interferometric measurement, LT-1 needs high accurate synchronization to guarantee the same working state of the two satellites in the data acquisition process, especially phase synchronization. An advanced non-interrupted phase synchronization scheme is proposed for LuTan-1[11,12]. The synchronization pulses are exchanged immediately after the ending time of the radar echo receiving window and before the starting time of the next pulse repetition interval, which will not interrupt the regular SAR operation and realize the high-accuracy phase synchronization. Moreover, LT-1 achieves a very high phase synchronization accuracy. To solve the contradiction between the short working time and the urgent need for large-scale global monitoring, a Non-linear wide-band FM (NLFM) transmit signal was proposed[13]. A satellite signal generator capable of generating arbitrary NLFM waveforms in orbit is equipped on LT-1, which can in-

*http://www.chinageoss.cn/tansat/index.html

crease the working time of satellites in a single orbit cycle by 22%[14].

SAR satellites have to sacrifice imaging swath width to achieve full polarization imaging capability, which reduces observation efficiency typically. To solve this problem, a series of new technologies such as multi-mode hybrid polarization and a new beamforming scheme have been proposed. SAR satellites' multi-polarization observation efficiency has improved, boosting the quantitative remote sensing capabilities of businesses like land, disaster relief, surveying and mapping, and forestry. Besides, a large number of promising observation products will be available, such as the single-pass polarimetry InSAR (Pol-InSAR) for forestry application, the hybrid polarimetric for land classification, *etc*. LT-1 will become the first SAR mission in the world with single-pass Pol-InSAR imaging capability. For example, forest biomass measurement is one of its most common applications, which provides an appropriate technological measurement for carbon cycle monitoring and further supports China's Carbon Dioxide Peaking and Carbon Neutrality plan.

Currently, Lutan-1 is undergoing on-orbit testing. Independent imaging experiments were performed for both LT-1 A and LT-1 B. The flight formation of Phase I is now in the process of being constructed, and it will be completed in three months. After LT-1 is put into use, it will provide a large amount of Earth observation data for scientific applications. It will drive the development of SAR system for acquiring multi-dimensional information on Earth's dynamic processes and monitoring the global environment.

4 Terrestrial Ecosystem Carbon Monitoring Satellite (TECMS)

Forest plays a crucial role in the carbon cycle and Earth system processes. Remote sensing is vital in quantifying forest carbon through different sensing capabilities (optical, radar, and LiDAR). According to the Application System Plan and Design of National Space Infrastructure (2015–2025), the Chinese Terrestrial Ecosystem Carbon Monitoring Satellite (TECMS) will be launched in the summer of 2022. TECMS is the first Chinese scientific satellite dedicated to comprehensively monitoring carbon storage in terrestrial ecosystems. It aims to monitor terrestrial ecosystems and provide measurements for major national ecological program evaluation.

TECMS has an orbit of 506 km with a 10:30 am operation time. The data coverage capacity is from –80° south to 80° north latitude. TECMS contains LiDAR and multi-angle optical (BRDF) sensors on board. There are 3 large footprint lasers with another 2 lasers as back-ups (see Fig.1). These five laser systems have a nominal footprint of 25 m. The full waveform data with 1 ns interval will be recorded. Each laser has a 35 Hz repeat frequency. The cross orbit distance among two adjacent laser footprints is about 8 km. The multi-angle optical (BRDF) observations consist of five VNIR cameras. Each camera contains 5 spectral bands with a 20 km swath. The nominal observation angles are 0°, ±28°, and ±50°. The spatial resolution is about 8 m.

The combination of multi-angle optical (BRDF) observations with waveform LiDAR remote sensing is unprecedented on board the same satellite. These laser waveforms provide detailed vertical structure informa-

Table 1 Imaging modes of LT-1. The achievable polarization, swath width, resolution and range of incidence angles are given in the description of each mode

Mode	Strip 1	Strip 2	Strip 3	Strip 4	Strip 5	Scan
Polarization	Single/Dual Pol., Compact Pol	Single/Dual Pol., Compact Pol	Quad Pol., Hybrid Pol	Quad Pol., Hybrid Pol	Single/Dual Pol., Compact Pol	Single/Dual Pol., Compact Pol
Resolution	3 m×3 m (Nominal)	12 m×12 m (Nominal)	3 m×3 m (Nominal)	6 m×6 m (Nominal)	24 m×24 m (Nominal)	30 m×30 m (Nominal)
Swath width	50 km	100 km	50 km	30 km	160 km	400 km
Incidence imaging angle	20°–53° (Imaging) 10°–60° (Extended)	20°–53°	10°–60°	13°–21°	15.7–30°	20°–49°
InSAR	20°–46°	20°–46°				

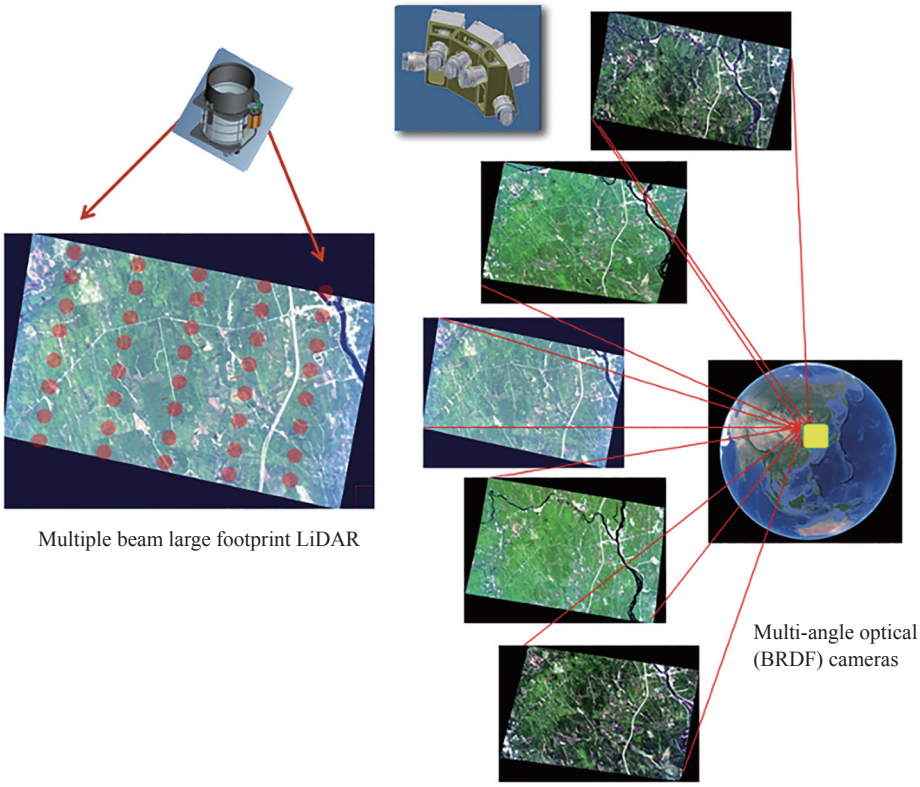

Fig. 1 LiDAR and multi-angle optical cameras configuration of the Chinese Terrestrial Ecosystem Carbon Monitoring Satellite (TECMS)

tion of forests as discrete footprints. The optical BRDF-imager extrapolates the laser height profiles to wall-to-wall biophysical vegetation maps. This innovative mission will significantly improve the capacity of forest carbon estimation.

5 Ocean Surface Current Multiscale Observation Mission (OSCOM)

Ocean Surface Current multiscale Observation Mission (OSCOM), is a satellite mission proposed to the Strategic Priority Program of Space Science (Phase III). The intensive study as a candidate mission has been supported by Chinese Academy of Sciences since 2020, and is under selection review now.

Motion is the essential state of the ocean. Ocean current is a primary physical parameter to describe the motion of the ocean. Global Ocean Surface Currents (OSC, including both speed and direction) play an important role in the momentum and energy coupling of multiscale ocean dynamics[15,16], air-sea exchange and interaction[17,18], ocean mass and energy transport and balance[19], global oceanic biochemical processes[20,21], and their effects on global changes[22–24]. The complete understanding of the spatial and temporal variation of multiscale ocean dynamics is a frontier to the development of ocean dynamics, air-sea interaction, marine ecological dynamics, biogeochemistry, and earth system modelling.

Firstly, ocean near-surface current has enormous energy, involving processes in multiple spatial and temporal scales (Fig.2)[25]. Nearly 90% of ocean kinetic energy clusters in mesoscale and sub-mesoscale, including near-inertial oscillations, fronts, mesoscale eddies, and sub-mesoscale processes[15]; secondly, OSC is a key element of the ocean water cycle, since it dramatically impacts the distribution and balance of the ocean temperature and salinity[26,27]; thirdly, feedback of the surface currents to the air-sea exchange through heat transports affects ocean surface fluxes and thermal equilibrium[28]; and fourthly, the surface currents determine the ocean nutrient transport, pollutant dispersion, sea ice drift, *etc*.[29–31], which seriously affects the biogeochemical cy-

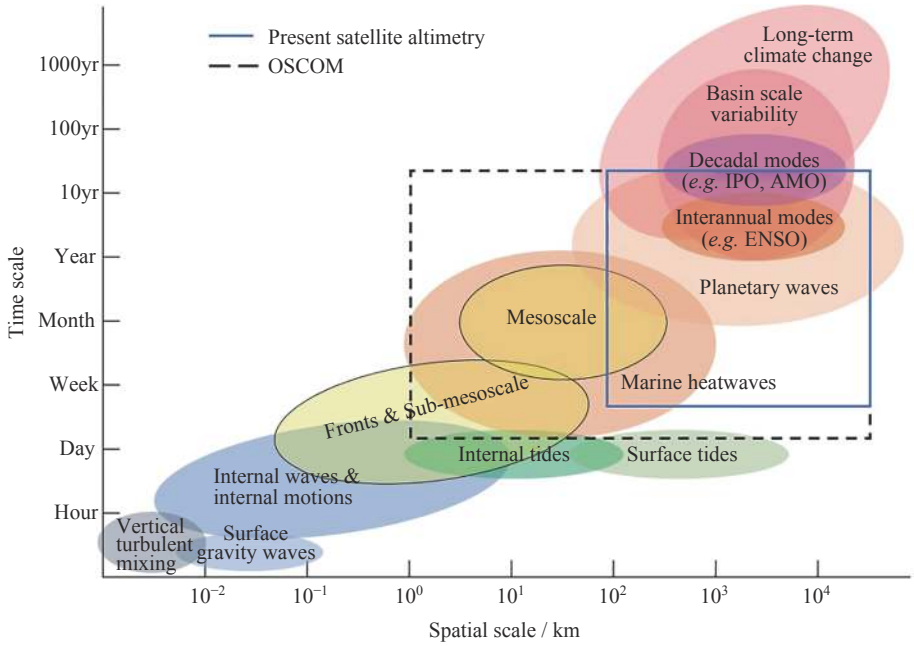

Fig. 2 Schematic diagram of multiscale ocean dynamics (updated from Chelton, 2011)

cle and ecosystem balance[20,21].

Satellite remote sensing is the most powerful tool for global ocean observations and monitoring. Presently, OSC is mainly derived from satellite altimeter data through the geostrophic equilibrium theory, only available to resolve quasi-geostrophic current at large- to meso-scale (>100 km) in the off-equatorial open oceans[32]. The quasi-geostrophic current in the middle and high latitudes, and, the ageostrophic and non-equilibrium processes and OSC in the equatorial and near-shore regions, especially in meso- to submeso-scales, are still rarely available globally[33]. This becomes a bottleneck impeding our understanding of the ocean dynamic processes.

Since the 2010 s, there has been a consensus among international scientific communities on the direct observation of the surface vector fields from space[24]. Scientific communities optimistically estimate that, by 2025, one and last most essential ocean environment measurement may become available — total ocean surface currents[34].

OSCOM will implement simultaneous observation of OSC, Ocean Surface Vector Winds (OSVW), and Ocean Surface Wave Spectrum (OSWS) by a Doppler Scatterometer (DOPS) (Fig.3). DOPS is a real-aperture radar with a dual-frequency (Ka+Ku) conically scanned rotating multi-pencil-beam antenna. By developing and exploiting combined ocean surface Doppler spectral, roughness spectral, and slope spectral models, OSC with high precision is to be retrieved from the measured Doppler frequency of backscattered signals (Table 2).

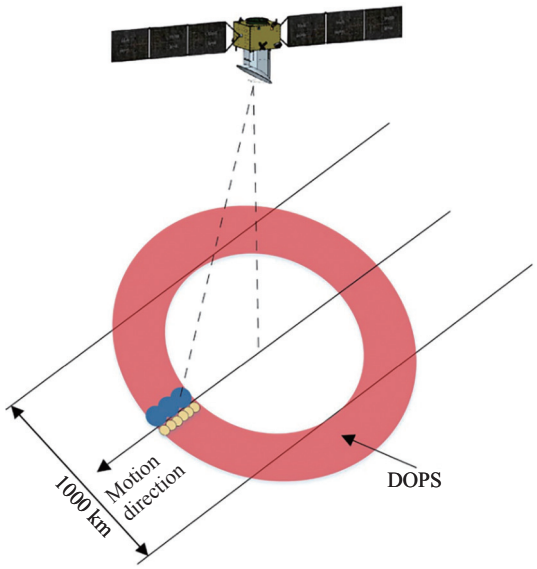

Fig. 3 Schematic diagram of the wide-swath OSCOM surface observations. The swath of OSCOM at the Earth's surface exceeds 1000 km in 650 km high orbit

The direct observation of the global OSC, OSVW, and OSWS, combined with other satellite observations (*e.g.*, high-resolution temperature and ocean color), will further facilitate the investigation and understanding of

Table 2 Expected performances of OSCOM

Variables	Spatial resolution	Accuracy/precision		Swath/temporal coverage
		Speed accuracy	Direction accuracy	
OSC	5 km	0.1 $m \cdot s^{-1}$	15°	>1000 km/ <3 days globally, mid-to-high latitude daily
OSVW	5 km	1.5 $m \cdot s^{-1}$	15°	
OSWS	10 km	10%@50–500 m wavelength		

ocean surface heat flux, carbon budget, and ocean biogeochemical cycle, and provide a novel pathway to data assimilation, coupling of General Circulation Models, and earth system modeling for ocean prediction and climate change.

5.1 Scientific Objectives

To directly observe global OSC at km scale (5–10 km), filling the gap of OSC observation in the space measurements.

To advance the research of ocean sub-mesoscale dynamics, multiscale processes, mass/energy exchanges between ocean and atmosphere, and biogeochemical cycles, promoting the development of theoretical research on ocean science and climate change.

To establish the foundation for numerical simulation of ocean non-equilibrium processes, providing theoretical and technical support for earth system modeling and Earth observation applications.

5.2 Expected Breakthroughs and Innovations

OSCOM will achieve a breakthrough in observing the global ocean's meso- and sub-mesoscale structures/processes from space directly, dedicated to the frontier of ocean multiscale dynamics and energetics based on satellite Doppler oceanography.

OSCOM will set a technical scheme to integrate OSC-OSVW-OSWS detection and inversion. Based on the sea surface Doppler velocity spectrum model, roughness spectrum model, and slope spectrum model, OSCOM will achieve simultaneous observations for a complete portrayal of ocean dynamic structure with a wide swath.

OSCOM will promote the development of many branches of Earth System Science, including physical oceanography, meteorology, biogeochemistry, climate dynamics, and geospatial information science, and improve the ability of earth system modeling to forecast global climate changes.

5.3 Key Technologies

OSCOM has been supported by an intensive pre-study project of candidate missions for Strategic Priority Program on Space Science II since 2020 for in-depth study and demonstration of scientific objectives, development of observation technologies, and retrieval models and techniques. Numerous projects have supported the research and development of the concept and technologies of DOPS since 2012, and an airborne technology verification campaign was completed in the summer of 2020.

The key enabling technologies include: integrated OSC-OSVW-OSWS measurement and retrieval models and techniques; space borne Ka-band power amplifier; and high-precision pointing measurement and determination. Pre-study and development of these technologies satisfy the TRL requirements to start the engineering phase of the mission.

6 Water Cycle Observatory from Space

The water cycle is the continuous movement of water within lands, oceans, and atmosphere. Terrestrial water cycle is a dynamic component of the global water cycle that exerts important controls over water, energy, and carbon fluxes at the land-atmosphere interface, where humans primarily operate, thereby playing an important role in water resources conservancy, meteorology and climatology, agriculture, ecology, and environment[35]. Space-based observations have been providing an unprecedented capacity in monitoring different components of the water cycle, such as the Global Precipitation Measurement (GPM) for precipitation[36], the Soil Moisture Ocean Salinity (SMOS) and Soil Moisture Active Passive (SMAP) for soil moisture[37,38], the Advanced Technology Microwave Sounder (ATMS) onboard NOAA-20 for water vapor[39], the Gravity Recovery and Climate Experiment (GRACE) for ground water storage[40], and the Surface Water and Ocean Topography (SWOT) for water surface elevations[41]. Such glob-

al observations from space should be secured and continued for the development of long-term consistent data record governing the terrestrial water cycle.

Since 2009 with the successful launch of the SMOS mission, it has been a golden age for the development of L-band radiometry from space, with the Aquarius launched in 2011 and SMAP launched in 2015. It has been proved that L-band radiometer and radar is an essential tool for monitoring soil moisture, vegetation water content, and landscape freeze-thaw processes. However, Aquarius is gone, and both SMOS and SMAP are aging. The Terrestrial Water Resources Satellite (TWRS) is a new Chinese mission under development focusing on space-based observation of terrestrial water components, that includes water stored in soil and vegetation, surface waters (rivers and inland water bodies), and solid waters (snow and ice), thus in support of estimation of terrestrial evapotranspiration. Initially, it is designed to have four payloads for the TWRS mission, including the L-band active-passive microwave imager, the multi-angle thermal infrared imager, the wide-swath multispectral camera, and the wide-swath programmable hyperspectral camera (see Table 3 for details). The TWRS mission is designed in Sun synchronous orbit, passing over the equator at 14:00 with an altitude of 680 km, thus, capturing the maximum evapotranspiration, which usually happens in early afternoon.

The L-band active-passive microwave imager is mainly used for the global mapping of soil moisture and its freeze-thaw status with a targeted spatial resolution about 5 km. Unlike the SMOS and SMAP missions, the L-band radiometer of TWRS is based on the one-dimensional synthetic aperture technology, which can reduce the complexity as compared to a two-dimensional radiometer of SMOS and avoid the risk of large antenna rotating (SMAP) to obtain high resolution observations in the cross-track direction. A synthetic aperture radar with higher spatial resolution than the radiometer is designed to share the reflector antenna towards soil moisture downscaling based on the synergy between active and passive microwave observations. However, this concept with incidence angle varying along the cross-track direction, raises new challenges including how to perform brightness temperature downscaling at variant incidence angles and how to reduce the dependence of soil moisture retrieval errors on incidence angle. This mission concept has been demonstrated in the Soil Moisture Experiment in the Luan River[42] focusing on specific challenges with the TWRS mission through an airborne simulator[43]. The active-passive approach for brightness temperature downscaling is found to be feasible with the airborne simulated observations of TWRS, the uncertainties caused by variant incidence angles can be suppressed by a downscaling method of spectral analysis [44]. It is indicated that the soil moisture retrieval is expected to have a satisfactory accuracy within 0.04 $m^3 \cdot m^{-3}$ under the incidence angle ranging from 30° to 50°, which would be adopted for the TWRS mission[45]. A novel soil moisture retrieval algorithm[46] is developed to enable the use of different combinations of microwave channels in terms of polarization, frequency, and incidence angles, and the algorithm for the TWRS mission would rely on polarization information with many other options including single-channel algorithm, dual-channel algorithm as adopted for the SMAP mission. In addition, the simultaneously retrieved vegetation optical depth has been found to be a good indicator of vegetation water content and water potential. With its multiple optical sensors including visible, near infrared, short wave infrared, and thermal infrared bands, the microwave-derived soil moisture can be further downscaled to an even higher spatial resolution for a much broader application.

The multi-angle thermal infrared imager allows retrieval of component temperatures of the land surface, which can improve the modeling of heat exchanges at the land-atmosphere interface. Component temperatures are essential for a better estimation of terrestrial evapotranspiration that deeply affects the water resources availability. The wide-swath multispectral camera is in support of mapping of dynamic changes of surface waters including rivers, lakes, and reservoirs, which are one of the most important resources for human survival and development. It can also be used for detecting the snow cover and glaciers due to the large difference in reflectance in the visible, near infrared and shortwave infrared regions of the spectrum. The programmable hyperspectral camera can be further used to estimate water quality parameters like sediment and carbon concentration and their spatial dynamics over water bodies. Therefore, the TWRS mission can provide a quite comprehensive observation of terrestrial water resources except for the water in the atmosphere and underground.

Table 3 Initial payload configuration of the Terrestrial Water Resources Satellite

L-band active-passive microwave imager		
Parameters	L-band radiometer	L-band radar
Frequency	1.413 GHz	1.26 GHz
Polarization	H, V, and T3	HH, VV, HV, and VH
Range of incidence angle	0°–40° or 30°–52° (to be adopted)	
Antenna	Parabolic cylinder antenna (12 m×10 m)	
Spatial resolution	18 km	1.5 km
Swath width	1000 km	
Wide-swath multispectral camera		
Parameters	Visible bands	Near-infrared bands
Spectral range	0.4–0.67 μm	0.85–0.97 μm
Spatial resolution	16 m	
Swath width	800 km	
Wide-swath programmable hyperspectral camera		
Parameters	Visible and near-infrared bands	Short-wave infrared bands
Spectral range	0.4–1.0 μm	1.0–1.68 μm
Spectral bands	128/64	80/40
Spatial resolution	25 m	
Swath width	120 km	
Multi-angle thermal infrared imager		
Spectral range	10.5–12.5 μm	
View angles	+48°, 0°, –31°	
Spatial resolution	100 m	
Swath width	1000 km	

Based on the planned TWRS mission, combined with China's existing Fengyun satellites and Haiyang satellites, it is expected to form an integrated capability of water cycle observatory from space with active-passive, multi-band remote sensing measurements.

7 Climate and Atmospheric Components Exploring Satellites (CACES)

Global climate change is one of the significant challenges of our time. A deeper understanding of how Greenhouse Gases (GHGs) impact and respond to climate change is one of the urgent scientific questions in Earth system science. Therefore, expanding the observational foundation for climate change studies with accurate, long-term, and consistent benchmark data is a fundamental need of climate science. The mission CACES, Climate and Atmospheric Components Exploring Satellites, focuses on benchmark climate variables and atmospheric composition observations from space to provide the essential atmospheric datasets for scientific research of global climate change.

The CACES satellite constellation consists of two Low-Earth-Orbit (LEO-LEO) satellites in sun-synchronous orbits: one transmitting (Tx) and one receiving (Rx) satellite (see Fig.4). The orbit altitudes for the Tx and Rx satellites are 500 km and 550 km, respectively. The Tx satellite actively sends signals through the atmosphere to the Rx satellite while the two types of satellites are counter-rotating to implement LEO-LEO occultation measurements. The satellites are designed to support autonomous on-orbit operations. The orbit information is exchanged through low-speed microwave communication between satellites, which supports the independent calculation of the occultation events during the satellites' rendezvous, the antenna or lens aiming of the Tx satellite and the Rx satellite is achieved through orbit atti-

tude maneuver.

CACES combines the microwave occultation (LMO) and the infrared-laser occultation (LIO) techniques by making breakthroughs in essential detection techniques for occultation measurements in the X/K microwave band and short-wave infrared (SWIR) band. It employs an LEO-to-LEO Microwave Occultation detection System (LMOS) and an Infrared-laser Occultation detention System (LIOS) on the constellation.

The LMOS is composed of a Transmitter (LMOS-T) instrument, a Receiver (LMOS-R) instrument, and a Precise Orbit Determination (POD) system. The LMOS is designed to employ X/K band signals to detect altitude and thermodynamic variables. The LMOS-T onboard the Tx satellite sends microwave signals through the atmosphere to the LMOS-R onboard the Rx satellite, during which the excess phases and the amplitude attenuations at different heights are measured. Based on these measurements, vertical profiles of refractivity and absorption are derived. This method can solve the temperature-humidity ambiguity and retrieve the temperature, pressure, and humidity profiles without auxiliary background information. The performance estimation of this 4-frequency LMOS has been conducted using quasi-realistic end-to-end simulations, and the results show that the retrieved temperature, pressure, and humidity profiles are generally unbiased and with minor standard deviations. The POD is the supporting payload for timing and navigation, which is also for the benefit of the LIOS payload.

The LIOS is also composed of a Transmitter (LIOS-T) and a Receiver (LIOS-R) instrument, which use infrared laser signals in the SWIR spectral region within the 2.0–2.5 μm band to provide profiling of GHG based on differential absorption measurements and species and further retrieve Line-of-sight (LOS) wind from through the spectral Doppler frequency shift. The infrared occultation system adopts the frequency stabilization technology of optical frequency combs to ensure the precision of laser wavelengths. The spatial heterodyne spectrometer in LIOS-R can achieve extremely high spectral resolution in a narrow field of view. Thus, the Earth's atmosphere is scanned from top to bottom, which enables high precision retrieval of vertical profiles of the atmospheric variables.

In practice, both the Tx and Rx satellites are equipped with a Fabry-Perot Interferometer (FPI)-based hyperspectral imager to fulfill local high-resolution monitoring of GHGs concentration (CO_2 and CH_4). The hyperspectral imager adopts a large-aperture transmission optical system, and the FPI enables high spectral resolution spectroscopy, which is featured by advantageous high spectral resolution, high spatial resolution, high throughput, lightweight, and miniaturization. Therefore, CACES can measure three-dimensional GHGs (CO_2, CH_4, H_2O, *etc.*) concentrations and LOS wind, simultaneously with thermodynamic variables (pressure, temperature, humidity), which also guarantees self-calibration and independence of the mission.

According to preliminary performance simulations, the CACES, when fulfilling its system requirements, can deliver its atmospheric profiles well within observation-

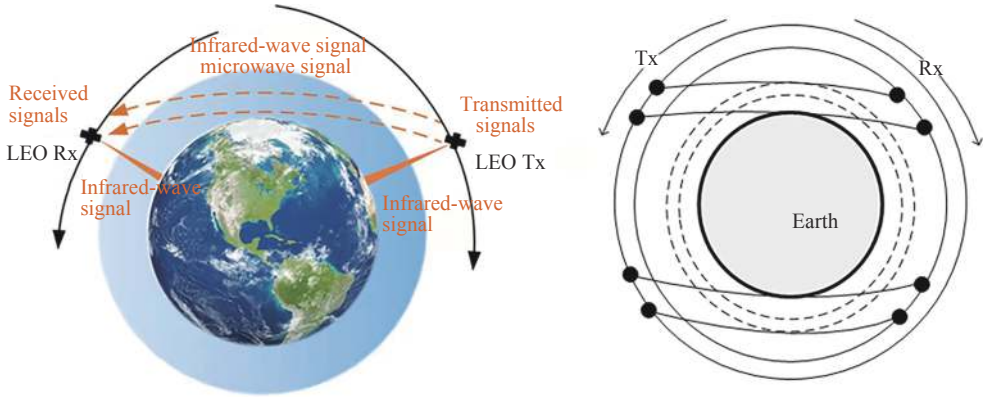

Fig. 4 Schematic view of the measurement concept of CACES, comprising the LIO, LMO components and the hyperspectral imager

al requirements and in most cases within target requirements. These results underline the potential of the CACES to provide benchmark measurements of unprecedented quality for addressing the climate and other science objectives. If implemented, CACES will provide all-day, accurate, and long-term stable data of essential climate variables with a high vertical resolution and achieve the great leap forward from one-dimensional measurements of GHGs column densities to three-dimensional detections. It will significantly drive the development of many branches of Earth system science research, thereby improving the ability of global change trends projection and a better understanding of the forcing and feedbacks that strongly link the atmosphere, human activities, and climate change. CACES will also provide a solid support for the carbon emission calculation in 2028 and China's targets of achieving a carbon peak by 2030 and carbon neutrality by 2060.

8 Conclusion

Currently, China has operated the second largest earth observation satellites in the world, and its satellite observation system of meteorology, oceanography, resources, environmental disaster reduction, and surveying/mapping has been continuously improved. In 2030, China will have around 30 Earth observation satellites in orbit, which may surpass the United States to become the world's largest. Space infrastructure development has laid the foundation for the development of space Earth Science from space. Space borne observations have been widely used in various branches of earth science, and have played a role that fundamentally changing the way of Earth science research. With the implementation of Earth science satellite missions, China will develop and cultivate a group of international frontiers. The progress of Earth Science from Space will continue to improve our understanding of climate change and comprehensively support the sustainable economic and social development goals.

References

[1] YANG D X, LIU Y, CAI Z, *et al.* First global carbon dioxide maps produced from TanSat measurements[J]. *Advances in Atmospheric Sciences*, 2018, **35**(6): 621-623

[2] LIU Y, WANG J, YAO L, *et al.* The TanSat mission: preliminary global observations[J]. *Science Bulletin*, 2018, **63**(18): 1200-1207

[3] LIU Y, WANG J, YAO L, *et al.* TanSat mission achievements: from scientific driving to preliminary observations[J]. *Chinese Journal of Space Science*, 2018, **38**(5): 627-639

[4] YANG D, BOESCH H, LIU Y, *et al.* Toward high precision XCO_2 retrievals from tansat observations: retrieval improvement and validation against TCCON measurements[J]. *Journal of Geophysical Research: Atmospheres*, 2020, **125**(22): e2020 JD032794

[5] YANG D X, LIU Y, BOESCH H, *et al.* A new TanSat XCO_2 global product towards climate studies[J]. *Advances in Atmospheric Sciences*, 2021, **38**(1): 8-11

[6] YANG D X, LIU Y, FENG L, *et al.* The first global carbon dioxide flux map derived from TanSat measurements[J]. *Advances in Atmospheric Sciences*, 2021, **38**(9): 1433-1443

[7] WANG H M, JIANG F, LIU Y, *et al.* Global terrestrial ecosystem carbon flux inferred from TanSat XCO_2 retrievals[J]. *Journal of Remote Sensing*, 2022, **2022**: 9816536

[8] DU S S, LIU L Y, LIU X J, *et al.* Retrieval of global terrestrial solar-induced chlorophyll fluorescence from TanSat satellite[J]. *Science Bulletin*, 2018, **63**(22): 1502-1512

[9] YAO L, YANG D X, LIU Y, *et al.* A new global solar-induced chlorophyll fluorescence (SIF) data product from TanSat measurements[J]. *Advances in Atmospheric Sciences*, 2021, **38**(3): 341-345

[10] YAO L, LIU Y, YANG D X, *et al.* Retrieval of solar-induced chlorophyll fluorescence (SIF) from satellite measurements: comparison of SIF between TanSat and OCO-2[J]. *Atmospheric Measurement Techniques*, 2022, **15**(7): 2125-2137

[11] JIN G D, LIU K Y, LIU D C, *et al.* An advanced phase synchronization scheme for LT-1[J]. *IEEE Transactions on Geoscience and Remote Sensing*, 2020, **58**(3): 1735-1746

[12] LIANG D, LIU K Y, ZHANG H, *et al.* The processing framework and experimental verification for the noninterrupted synchronization scheme of LuTan-1[J]. *IEEE Transactions on Geoscience and Remote Sensing*, 2021, **59**(7): 5740-5750

[13] WANG W, WANG R, ZHANG Z M, *et al.* First demonstration of airborne SAR with nonlinear FM chirp waveforms[J]. *IEEE Geoscience and Remote Sensing Letters*, 2016, **13**(2): 247-251

[14] JIN G D, DENG Y K, WANG R, *et al.* An advanced nonlinear frequency modulation waveform for radar imaging with low sidelobe[J]. *IEEE Transactions on Geoscience and Remote Sensing*, 2019, **57**(8): 6155-6168

[15] FERRARI R, WUNSCH C. Ocean circulation kinetic energy: reservoirs, sources, and sinks[J]. *Annual Review of Fluid Mechanics*, 2009, **41**: 253-282

[16] CHEN R, FLIERL G R, WUNSCH C. A description of local and nonlocal eddy–mean flow interaction in a global eddy-permitting state estimate[J]. *Journal of Physical Oceanography*, 2014, **44**(9): 2336-2352

[17] NAKAMURA H, SAMPE T, GOTO A, *et al.* On the im-

portance of midlatitude oceanic frontal zones for the mean state and dominant variability in the tropospheric circulation[J]. *Geophysical Research Letters*, 2008, **35**(15): L15709

[18] SU Z, WANG J B, KLEIN P, *et al*. Ocean submesoscales as a key component of the global heat budget[J]. *Nature Communications*, 2018, **9**(1): 775

[19] BOCCALETTI G, FERRARI R, ADCROFT A, *et al*. The vertical structure of ocean heat transport[J]. *Geophysical Research Letters*, 2005, **32**(10): L10603

[20] LEGECKIS R, BROWN C W, BONJEAN F, *et al*. The influence of tropical instability waves on phytoplankton blooms in the wake of the Marquesas Islands during 1998 and on the currents observed during the drift of the Kon-Tiki in 1947[J]. *Geophysical Research Letters*, 2004, **31**(23): L23307

[21] YODER J A, DONEY S C, SIEGEL D A, *et al*. Study of marine ecosystems and biogeochemistry now and in the future: examples of the unique contributions from space[J]. *Oceanography*, 2010, **23**(4): 104-117

[22] DOHAN K, MAXIMENKO N. Monitoring ocean currents with satellite sensors[J]. *Oceanography*, 2010, **23**(4): 94-103

[23] DOHAN K. Ocean surface currents from satellite data[J]. *Journal of Geophysical Research: Oceans*, 2017, **122**(4): 2647-2651

[24] LEE T, HAKKINEN S, KELLY K, *et al*. Satellite observations of ocean circulation changes associated with climate variability[J]. *Oceanography*, 2010, **23**(4): 70-81

[25] TALLEY L D, PICKARD G L, EMERY W J, *et al*. Descriptive Physical Oceanography: An Introduction[M]. 6 th ed. Boston: Academic Press, 2011

[26] GORDON C, COOPER C, SENIOR C A, *et al*. The simulation of SST, sea ice extents and ocean heat transports in a version of the Hadley Centre coupled model without flux adjustments[J]. *Climate Dynamics*, 2000, **16**(2/3): 147-168

[27] YU L S. A global relationship between the ocean water cycle and near-surface salinity[J]. *Journal of Geophysical Research: Oceans*, 2011, **116**(C10): C10025

[28] YU L S, WELLER R A. Objectively analyzed air-sea heat Fluxes for the global ice-free oceans (1981–2005)[J]. *Bulletin of the American Meteorological Society*, 2007, **88**(4): 527-540

[29] LETSCHER R T, PRIMEAU F, MOORE J K. Nutrient budgets in the subtropical ocean gyres dominated by lateral transport[J]. *Nature Geoscience*, 2016, **9**(11): 815-819

[30] MAES C, GRIMA N, BLANKE B, *et al*. A surface "super-convergence" pathway connecting the South Indian Ocean to the subtropical South Pacific gyre[J]. *Geophysical Research Letters*, 2018, **45**(4): 1915-1922

[31] VAN SEBILLE E, GRIFFIES S M, ABERNATHEY R, *et al*. Lagrangian ocean analysis: fundamentals and practices[J]. *Ocean Modelling*, 2018, **121**: 49-75

[32] CHELTON D B, SCHLAX M G, SAMELSON R M. Global observations of nonlinear mesoscale eddies[J]. *Progress in Oceanography*, 2011, **91**(2): 167-216

[33] QIU B, CHEN S M, KLEIN P, *et al*. Reconstructing upper-ocean vertical velocity field from sea surface height in the presence of unbalanced motion[J]. *Journal of Physical Oceanography*, 2020, **50**(1): 55-79

[34] FREEMAN A, ZLOTNICKI V, LIU T, *et al*. Ocean measurements from space in 2025[J]. *Oceanography*, 2010, **23**(4): 144-161

[35] GIROTTO M, RODELL M. Terrestrial water storage[M]//MAGGIONI Y, MASSARI C. Extreme Hydroclimatic Events and Multivariate Hazards in A Changing Environment: A Remote Sensing Approach. Amsterdam: Elsevier, 2019: 41-64

[36] SMITH E A, ASRAR G, FURUHAMA Y, *et al*. International Global Precipitation Measurement (GPM) program and mission: an overview[M]//LEVIZZANI V, BAUER P, TURK F J. Measuring Precipitation from Space: EURAINSAT and the Future. Dordrecht: Springer, 2007. 611-653

[37] KERR Y H, WALDTEUFEL P, WIGNERON J P, *et al*. The SMOS mission: new tool for monitoring key elements of the global water cycle[J]. *Proceedings of the IEEE*, 2010, **98**(5): 666-687

[38] ENTEKHABI D, NJOKU E G, O'NEILL P E, *et al*. The Soil Moisture Active Passive (SMAP) mission[J]. *Proceedings of the IEEE*, 2010, **98**(5): 704-716

[39] WENG F Z, YANG H, ZOU X L. On convertibility from antenna to sensor brightness temperature for ATMS[J]. *IEEE Geoscience and Remote Sensing Letters*, 2013, **10**(4): 771-775

[40] TAPLEY B D, BETTADPUR S, RIES J C, *et al*. GRACE measurements of mass variability in the Earth system[J]. *Science*, 2004, **305**(5683): 503-505

[41] BIANCAMARIA S, LETTENMAIER D P, PAVELSKY T M. The SWOT mission and its capabilities for land hydrology[M]//CAZENAVE A, CHAMPOLLION N, BENVENISTE J, *et al*. Remote Sensing and Water Resources. Cham: Springer, 2016: 117-147

[42] ZHAO T J, SHI J C, LV L Q, *et al*. Soil moisture experiment in the Luan River supporting new satellite mission opportunities[J]. *Remote Sensing of Environment*, 2020, **240**: 111680

[43] SUN Yanlong, ZHAO Tianjie, LI Enchen, *et al*. Radiometer calibration of airborne L-band active and passive microwave detector[J]. *National Remote Sensing Bulletin*, 2021, **25**(4): 918-928

[44] GUO P, ZHAO T J, SHI J C, *et al*. Assessing the active-passive approach at variant incidence angles for microwave brightness temperature downscaling[J]. *International Journal of Digital Earth*, 2021, **14**(10): 1273-1293

[45] ZHAO T J, HU L, SHI J C, *et al*. Soil moisture retrievals using L-band radiometry from variable angular ground-based and airborne observations[J]. *Remote Sensing of Environment*, 2020, **248**: 111958

[46] ZHAO T J, SHI J C, ENTEKHABI D, *et al*. Retrievals of soil moisture and vegetation optical depth using a multi-channel collaborative algorithm[J]. *Remote Sensing of Environment*, 2021, **257**: 112321